Optimizing utilization efficiencies in electronegative discharges: The importance of the impedance phase angle

W. R. Entley,[a] J. G. Langan, and B. S. Felker
Air Products and Chemicals, Inc., Allentown, Pennsylvania 18195

M. A. Sobolewski
National Institute of Standards and Technology, Gaithersburg, Maryland 20899

(Received 2 July 1999; accepted for publication 5 August 1999)

We have investigated the operating conditions that result in the greatest utilization efficiencies (UEs) of NF_3, CF_4, and C_2F_6 in a capacitively coupled GEC reference cell. We have also independently measured the rf electrical characteristics and optical emission spectra of the plasmas. To avoid inadvertently attributing changes in the UE, discharge impedance, rf currents, or atomic emission intensities to parasitic losses in the matching network or rf delivery system, the rf generator was adjusted to ensure that the same amount of power was dissipated within each discharge. For the NF_3 plasmas, argon was used as a diluent and both the NF_3 concentration and reactor pressure were varied. For the CF_4 and C_2F_6 based plasmas, the gas compositions were fixed (86 mol % CF_4/O_2 and 50 mol % C_2F_6/O_2) and the reactor pressure was varied. The greatest NF_3 UEs occurred within a narrow range of NF_3 partial pressures. The greatest CF_4 and C_2F_6 UEs occurred within a narrow range of reactor pressures. For all mixtures, operating conditions that yielded the highest UEs also yielded the brightest plasmas, the lowest impedance magnitudes, the greatest fraction of current flowing to the grounded electrode, and impedance phase angles within a narrow window centered near $\phi_{pe}=-40°$. Within this region, plasma power is most efficiently utilized to dissociate the source gas and excite the atoms that emit light. Collapsed plasmas, observed for high pressure highly electronegative conditions, exhibited very low UEs. At optimal operating conditions the UE of the fluorinated source gases were found to decrease in the order: $NF_3>C_2F_6>CF_4$. The results of this study suggest that the baseline corrected fluorine atom emission intensity (703.7 nm), the magnitude of the discharge impedance, or phase angle of the discharge impedance could be monitored to determine the relative fluorinated source gas UE in an arbitrary plasma reactor as the operating conditions are varied. The concept of an ideal NF_3 partial pressure could prove to be a useful strategy to prevent the formation of collapsed plasmas at high reactor pressures while maintaining high NF_3UEs. © *1999 American Institute of Physics.*
[S0021-8979(99)08821-0]

I. INTRODUCTION

Perfluorocompounds (PFCs) such as NF_3, C_2F_6, and CF_4 are widely used for the removal of residue following plasma enhanced chemical vapor deposition (PECVD).[1–6] In PECVD, plasma excitation of source gas(es) is used to deposit dielectric or metallic thin films on silicon wafers at relatively low temperatures (400 °C). However, deposition occurs not only on the wafer, but also on the exposed internal surfaces of the PECVD chamber. This residue must be removed in order to minimize potential yield loss due to microcontamination and to maintain process integrity. *In situ* plasma removal of the residue is carried out by excitation of a fluorinated source gas which generates reactive fluorine atoms and radicals. These species react with the deposition residue forming volatile produces which are evacuated from the chamber. Although PFCs are used for other plasma processing applications, PECVD chamber cleaning accounts for approximately 60%–95% of the use of these gases within the semiconductor industry.[1]

Concern over the global warming potential and long atmospheric lifetimes of PFCs has initiated worldwide efforts to minimize their release into the atmosphere.[1,7] Of particular interest to integrated circuit manufacturers are strategies targeted at minimizing PECVD chamber cleaning emissions. One of the most promising is process optimization, in which the operating conditions of the reactor are adjusted to achieve the highest PFC utilization efficiency (the percentage of influent PFC consumed during the clean).[1,7] Although this strategy has been successfully utilized in commercial reactors, much less work has been done to fundamentally understand the operating conditions that result in the greatest fluorinated source gas utilization efficiency (UE).[1,6,7,8] In this work we systematically determine the operating conditions that yield the highest UEs for PFCs commonly used in PECVD chamber cleaning (NF_3, CF_4, and C_2F_6). All experiments are carried out in a rf capacitively coupled GEC reference cell.[9] For the NF_3 based plasmas, argon is used as a diluent and both the NF_3 concentration and the reactor pressure are varied. For the CF_4 and C_2F_6 based plasmas, the gas compositions are fixed (86 mol % CF_4/O_2 and 50 mol %

[a]Electronic mail: entleywr@apci.com

C_2F_6/O_2) and the reactor pressure is varied. To determine how the discharge impedance and the atomic emission intensities change within the experimental matrix, we measure the rf electrical characteristics (i.e., current and voltage waveforms at the powered electrode and the current waveform at the grounded electrode) and optical emission spectra of the plasmas. From the rf electrical measurements we also calculate the actual power dissipated within the discharge. To avoid inadvertently attributing changes in the UE, discharge impedance, rf currents, or atomic emission intensities to parasitic losses in the matching network or rf delivery system, the rf generator was adjusted to ensure that the same amount of power was dissipated within each discharge. This last step is critical since as little as 9% of available rf power may be dissipated within high pressure highly electronegative discharges.[10–14]

Previously we have shown a strong correlation between different regions of electrical behavior in fluorinated gas discharges and the mechanisms by which power is consumed within these regions.[15] At low pressures a region characterized by capacitive impedance is observed in which nearly all of the plasma power is consumed by ions in the powered electrode sheath. Increasing the pressure within this region results in a decrease in the magnitude of the discharge impedance, a decrease in the amount of power consumed by the ions in the sheath, and an increase in the amount of power consumed by the electrons in the bulk glow. At high pressures a region exhibiting inductive character is observed. Increasing the pressure within this region increases the magnitude of the discharge impedance and causes the glow to contract and eventually collapse to a small bright ring along the edge of the powered electrode and its ground shield. The inductive phase angles observed in this high pressure highly electronegative region may be an indication of absorption of power by ions in the bulk glow.[13,15,16] Between these two extremes lies a transition region where the brightest plasmas with the lowest discharge impedances are observed. Regardless of the gas composition the transition region always occurs near an impedance phase angle of $\phi_{pe}=-40°$.[14,15] In this work we have chosen to monitor the source gas UE as a function of impedance phase angle. By correlating the UE and phase angle we hope to gain further insight into the fundamental mechanisms occurring in electronegative plasma processes. Other investigators have used similar analyses to correlate changes in plasma parameters with the different mechanisms by which rf power is absorbed in electronegative discharges as the operating conditions are varied.[14,17]

II. EXPERIMENT

All experiments were carried out in a 13.56 MHz capacitively coupled gaseous electronics conference (GEC) reference cell.[9] Figure 1 shows a diagram of the cell and its electrical connections. The chamber is constructed of 304 stainless steel. The two piece electrodes are 10 cm in diameter, and consist of an outer 6061 aluminum surface fastened via stainless steel screws over an inner stainless steel backing which is internally cooled by the circulation of deionized water at 21 °C; an indium gasket separates the aluminum and stainless steel surfaces. Both electrodes are electrically isolated from the chamber via Teflon insulators and surrounded by stainless steel ground shields. The interelectrode spacing is 2.3 cm. Experiments were carried out with the top electrode grounded. Radio frequency power was delivered to the bottom electrode at 13.56 MHz via a rf plasma products generator (RF-5S)[18] coupled to the lower electrode through a manually tuned π-type matching network (ENI MW-5) and an inductive shunt circuit[9,19] that was tuned to 13.56 MHz.

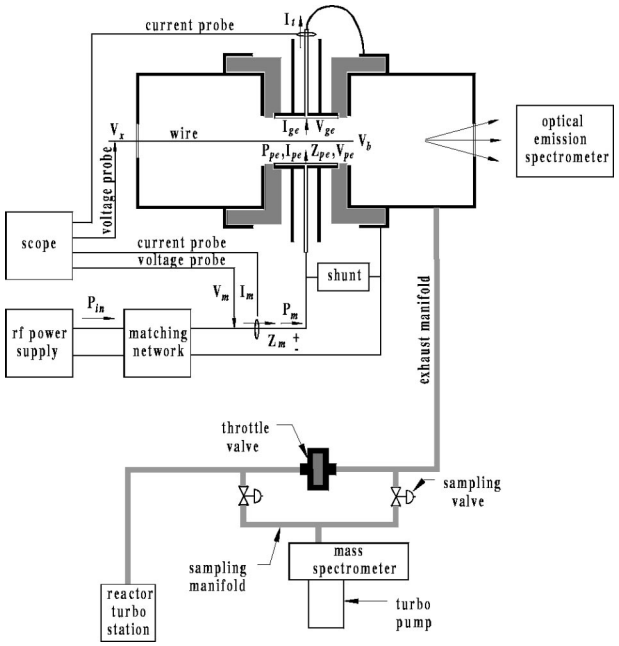

FIG. 1. Schematic of GEC cell showing the placement of the mass spectrometer, optical emission spectrometer, and the current and voltage probes. The figure also defines the various electrical parameters.

Argon (Air Products VSLI Grade), NF_3 (Air Products Megaclass® Grade), O_2 (Air Products Research Grade), C_2F_6 (Air Products Electronics Grade), and CF_4 (Air Products Semiconductor Grade) were used as received without further purification. Gases enter the cell via a showerhead arrangement of holes in the upper electrode; the flow rates are controlled with either MKS 2159 (Ar, NF_3, O_2, and C_2F_6) or MKS 1159 (CF_4) mass flow controllers. Feed gas concentrations are calculated from their relative volumetric flow rates. Constant chamber pressure is maintained by a downstream throttle valve (MKS 253A) controlled via a signal from an MKS 128 Baratron capacitance manometer. A corrosive series hybrid pump (Pfeiffer Vacuum Technologies, Inc. TPU 180 HC) exhausts the system.

The flow rate of NF_3 was fixed at 12.5 sccm (9.3 μmoles/s) for each experiment. At each reactor pressure the flow rate of argon was varied from 3 to 56.9 sccm in order to vary the concentration of NF_3 in the feed gas mixture from 81 to 18 mol %. C_2F_6 experiments were run at a total fixed flow rate of 26.5 sccm, consisting of 12.5 sccm of C_2F_6, 12.5 sccm of O_2, and 1.5 sccm of Ar. CF_4 experiments were run at a total fixed flow rate of 16.0 sccm, consisting of 12.5 sccm of CF_4, 2.0 sccm of O_2, and 1.5 of Ar. Only the reactor pressure was varied in the C_2F_6 and CF_4 experiments; Ar

was added for the purposes of mass spectrometry and optical emission spectroscopy. For every experiment described in this article the setting on the rf generator was adjusted to ensure that 35 ± 0.5 W of power was dissipated within the plasma. The procedure of fixing the plasma power (P_{pe}) to 35 ± 0.5 W eliminates the effect of any losses in the rf power supply/matching network and cell parasitics associated with a given source gas and reactor pressure setting.

Electrical measurements were carried out as previously described.[15] After characterizing the cell parasitics, an equivalent circuit model was used to convert the measured signals (I_m, V_m, and I_t) into the signals of interest (I_{pe}, V_{pe}, I_{ge}, and V_{ge}).[19,20] Here I_{pe} is the current flowing from the surface of the powered electrode into the plasma, V_{pe} is the rf voltage on the surface of the powered electrode, I_{ge} is the current flowing from the plasma to the surface of the grounded electrode, and V_{ge} is the rf voltage on the surface of the grounded electrode (which is not zero due to the parasitic series resistance and self inductance of the grounded electrode assembly). The voltages are referenced to the ground shield of the powered electrode. Only the Fourier components of the measured signals at 13.56 MHz are reported here. Harmonic components were also recorded, but previous experiments under similar conditions showed that they carried no significant power.[15]

Once V_{pe} and I_{pe} are determined, both the power flowing from the surface of the powered electrode into the discharge (P_{pe}), and the combined impedance of everything downstream of the powered electrode (Z_{pe}) can be obtained. These quantities are given by the following equations, where ϕ_{pe} is the phase angle of Z_{pe} (i.e., the phase of V_{pe} with respect to I_{pe}):

$$P_{pe}=\frac{V_{pe}I_{pe}}{2}\cos\phi_{pe}, \tag{1}$$

$$Z_{pe}=\frac{V_{pe}}{I_{pe}}. \tag{2}$$

The impedance Z_{pe} includes the impedance of the plasma sheaths and the impedance of the bulk plasma; no attempt was made to numerically separate the impedance of the sheaths from the impedance of the plasma.

Plasma processes were monitored with a UTI 100C quadrupole mass spectrometer fitted with a low pressure sampling system. A differentially pumped sampling manifold was installed to ensure a fast sampling response; samples of the neat plasma effluent were extracted upstream of the throttle valve (Fig. 1). To avoid problems associated with the buildup of source gas residue in the mass spectrometer, the majority of the experiments were carried out with the mass spectrometer heated to 120 °C. This procedure not only has the advantage of removing the background contaminants, but also inhibits surface adsorption of the gases of interest.[21]

Relative partial pressures of Ar, NF_3, CF_4, and C_2F_6 were determined by monitoring the intensity of the following ion fragments in the mass spectrometer: Ar^+(40 m/e), NF_2^+(52 m/e), CF_3^+(69 m/e), and $C_2F_5^+$ (119 m/e). The choice of the NF_2^+ (52 m/e) peak over the NF_3^+ (71 m/e) peak was dictated by its greater precision. Although the formation of plasma generated N_2F_4 in the discharge would preclude the use of the NF_2^+ (52 m/e) peak to calculate the utilization efficiency of NF_3, we found no evidence for its formation; the ratio of the NF_2^+ (52 m/e) peak to the NF_3^+ (71 m/e) peak remained constant throughout the entire experimental matrix, as observed previously.[22] For the NF_3 and CF_4 based plasmas, a mass range of 4–84 amu was scanned, while for C_2F_6 based discharges a mass range of 3–143 amu was scanned. Full range mass spectra were acquired for each experimental point, at the specified gas flow rates and pressure, with the radio frequency power off (rfOFF) and with the radio frequency power on (rfON).

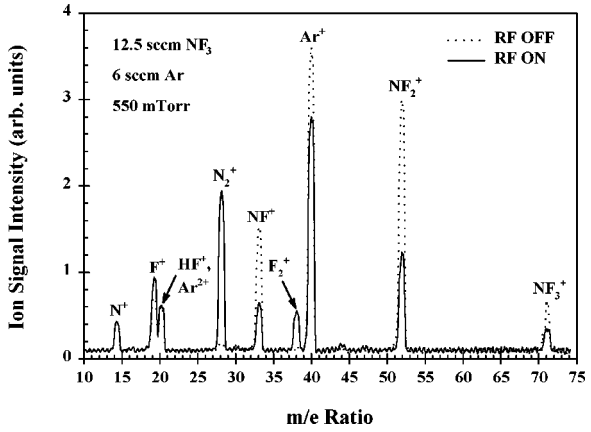

FIG. 2. Typical full range mass spectra acquired for a 68 mol % NF_3/Ar gas mixture at 550 mtorr with the applied rf power off (rfOFF) and with the applied rf power on (rfON). Upon application of the rf power a significant decrease is observed in nearly all of the original ion signal intensities and new gaseous species are formed in the discharge (N_2, F_2).

Figure 2 compares the rfON and rfOFF mass spectra for a 68 mol % NF_3/Ar discharge at a reactor pressure of 550 mTorr (73.3 Pa). Upon application of the rf power, the source gas is dissociated and a significant decrease is observed in nearly all of the original ion signal intensities and new ion signals corresponding to F_2^+ (m/e=38) and N_2^+ (m/e=28) are observed. Of particular interest is the decrease in the Ar^+ (m/e=40) ion signal intensity. Since the feed gas flow rates are fixed and the reactor pressure is held constant by means of a variable throttle valve, the decrease in the Ar^+ (m/e=40) ion signal intensity is due to an increase in the total molar flow rate of exhaust gases as the molecular source gas is fragmented and new gaseous species are formed (e.g., F_2 and N_2). This increase in the total molar gas flow rate decreases the partial pressure of Ar in the reactor and consequently decreases its ion signal intensity. This effect also contributes to the decrease in the ion signal intensities of the fluorinated gas fragments. Thus, upon application of the rf power, the decrease in the intensity of the NF^+ (m/e=33), NF_2^+=(m/e=52), and NF_3^+=(m/e=71) peaks is due not only to the consumption of the source gas, but also to the increase in the total molar flow rate of exhaust gases.

Source gas UEs were calculated from Eq. (3):

$$\mathrm{UE}(\%)=\left[1-\left(\frac{I_{SG}(\mathrm{rfON})}{I_{40}(\mathrm{rfON})}\,\frac{I_{40}(\mathrm{rfOFF})}{I_{SG}(\mathrm{rfOFF})}\right)\right]100, \tag{3}$$

where I_{SG} is the ion signal intensity of the appropriate molecular source gas fragment and I_{40} is the ion signal intensity of Ar^+.[23] In Eq. (3) the ion signal intensity of argon is used as an internal standard to correct for the increased molar flow rate of exhaust gases upon generation of a plasma. This correction is critical when sampling the neat plasma effluent from a reactor; without the use of an internal standard our calculated UEs were overestimated by as much as 13%. Unless otherwise shown, the reproducibility of the calculated UEs are approximately ±4%.

In the C_2F_6/O_2 discharges the ratio of the m/e=69 signal (CF_3^+) to the m/e=119 ($C_2F_5^+$) signal with rfON was significantly larger compared to the ratio with rfOFF. The increase of this ratio with rfON is due to the formation of plasma generated CF_4 which contributes to the intensity of the m/e=69 signal, but not to the intensity of the m/e=119 signal.[1,6] Since the ratio of the m/e=69 ion signal intensity to the m/e=119 ion signal intensity arising from C_2F_6 is the same for both rfON and rfOFF, the C_2F_6 contribution to the intensity of the rfON m/e=69 signal can be calculated from the following relationship:

$$\left[\frac{I_{69}(C_2F_6)}{I_{119}(C_2F_6)}\right]\text{rfON}=\left[\frac{I_{69}(C_2F_6)}{I_{119}(C_2F_6)}\right]\text{rfOFF}. \tag{4}$$

The plasma generated CF_4 contribution to the intensity of the rfON m/e=69 signal is obtained by subtracting the calculated C_2F_6 rfON m/e=69 signal intensity from the total intensity of the rfON m/e=69 signal. The rate of information of plasma generated CF_4 can then be obtained from the following equation:

$$[CF_4(\text{sccm})]_{\text{rfON}}=\frac{[I_{69}(CF_4)]_{\text{rfON}}}{[I_{69}(C_2F_6)]_{\text{rfON}}}\frac{\varepsilon(CF_4)}{\varepsilon(C_2F_6)}\times[C_2F_6(\text{sccm})]_{\text{rfON}}, \tag{5}$$

where the term $\varepsilon(CF_4)/\varepsilon(C_2F_6)$ accounts for differences in the ionization efficiencies and mass spectrometer responses of the C_2F_6 and CF_4. The $\varepsilon(CF_4)/\varepsilon(C_2F_6)$ term was evaluated from calibration data[24] and the $[C_2F_6(\text{sccm})]_{\text{rfON}}$ term was evaluated from the calculated utilization efficiency of the process. Equation (5) was used to calculate the rate of formation of the plasma generated CF_4 in all of the C_2F_6/O_2 plasmas.

Optical emission spectra were collected with a SC Technology Model PCM-401 full wavelength spectrometer utilizing a fiber optic cable to collect light from the plasma. The fiber optic cable was mounted on a quartz window and centered between the powered and grounded electrodes. Because the fiber optic cable accepted light over a wide range of incident angles, the emission intensities were spatially averaged. The instrument grating was adjusted to collect emission intensities between 577 and 877 nm, at a resolution of 0.5 nm. Emission intensities were time averaged. The baseline corrected peak intensities at 703.7, 750.4, and 777.4 nm were used to monitor the relative concentrations of the excited state fluorine, argon, and oxygen atoms in the discharge, respectively.

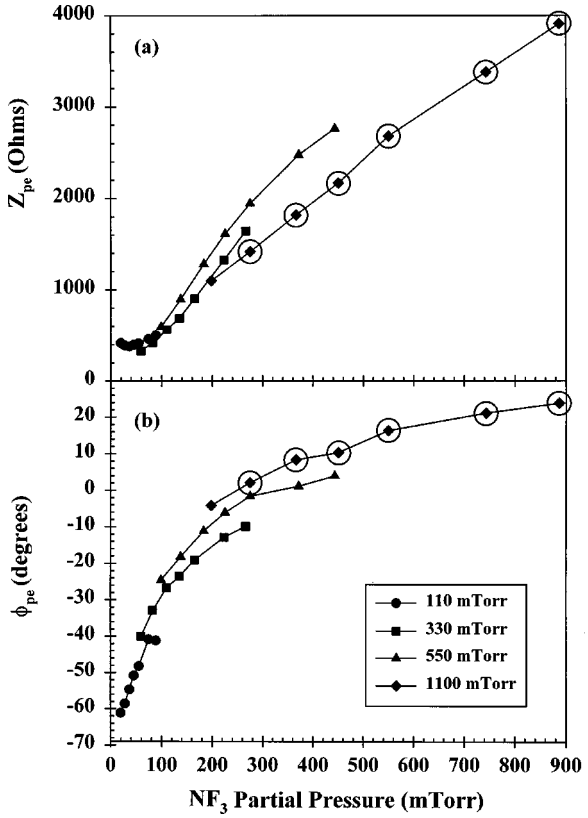

FIG. 3. Plasma impedance magnitude (a) and phase angle (b) for the NF_3/Ar plasmas as a function of the NF_3 partial pressure, where the NF_3 partial pressure in the reactor is calculated *prior* to initiating a discharge. The circle data points represent collapsed plasmas. All data points correspond to a fixed plasma power (P_{pe}) of 35.0±0.5 W and 12.5 sccm of NF_3; at each reactor pressure (given in the legend) the mixtures range in composition from 18 to 81 mol % NF_3.

III. RESULTS

Impedance measurements as a function of NF_3 concentration were obtained at each reactor pressure. Both the impedance magnitude, $|Z_{pe}|$, and the impedance phase angle, ϕ_{pe}, are strong functions of the reactor pressure and NF_3 concentration (i.e., the NF_3 partial pressure in the reactor *prior* to initiating a discharge). Figures 3(a) and 3(b) show $|Z_{pe}|$ and ϕ_{pe} as a function of the NF_3 partial pressure at each reactor pressure, respectively. At 110 mTorr $|Z_{pe}|$ initially decreases, reaches a shallow minimum, and then increases as the NF_3 partial pressure is increased. At this pressure $|Z_{pe}|$ is small (<550 Ω) at both low and high NF_3 partial pressures. At higher reactor pressures $|Z_{pe}|$ increases sharply as the NF_3 partial pressure is increased. Throughout the entire experimental matrix, increasing the NF_3 partial pressure results in a more positive phase angle. At the highest NF_3 partial pressure $|Z_{pe}|$ is very large (>2000 Ω), and the phase angle is inductive (i.e., positive). Our results are consistent with impedance measurements of NF_3/Ar plasmas previously reported in the GEC cell.[15]

The circled data points in Fig. 3 represent collapsed plasmas. Collapsed plasmas are glows which are largely confined to a small region along the edge of the powered electrode and its ground shield, the balance of the electrode gap glowing very dimly or not at all. The formation of collapsed plas-

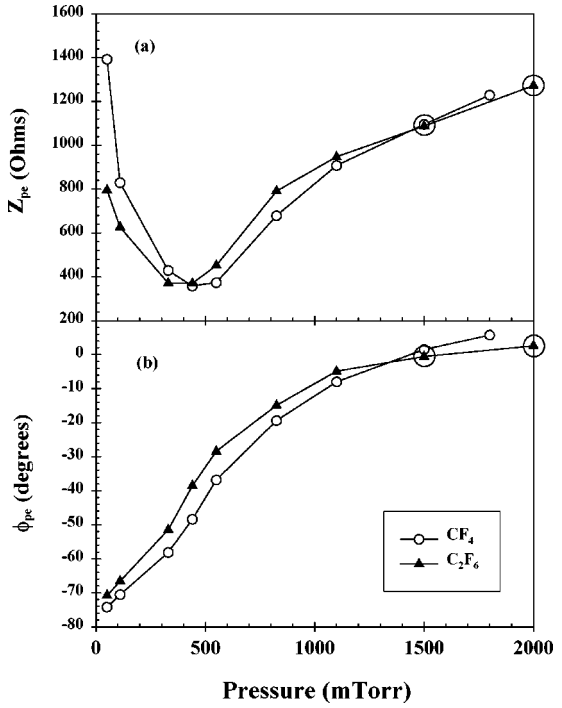

FIG. 4. Plasma impedance magnitude (a) and phase angle (b) for the 86 mol % CF_4/O_2 and 50 mol % C_2F_6/O_2 plasmas as a function of the reactor pressure. The circled data points represent collapsed plasmas. All data points correspond to a fixed plasma power (P_{pe}) of 35.0±0.5 W and 12.5 sccm of CF_4 or C_2F_6.

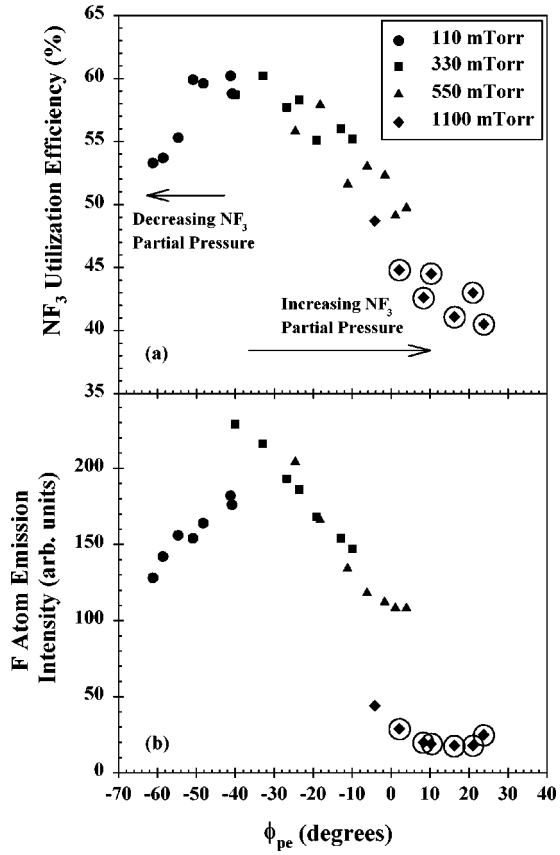

FIG. 5. NF_3 utilization efficiency (a) and baseline corrected fluorine atom emission intensity (b) for the NF_3/Ar plasmas as a function of the complex impedance phase angle. At impedance phase angles less that $\phi_{pe} = -40°$ the NF_3 UE and fluorine atom emission intensity decrease as the NF_3 partial pressure is decreased. At impedance phase angles greater than $\phi_{pe} = -40°$ the NF_3 UE and fluorine atom emission intensity decrease as the NF_3 partial pressure is increased. The circled data points represent collapsed plasmas. All data points correspond to a fixed plasma power (P_{pe}) of 35.0±0.5 W and 12.5 sccm of NF_3; at each reactor pressure the mixtures range in composition from 18 to 81 mol % NF_3.

mas in electronegative discharges in the GEC cell has been described in detail, and its favored by high concentrations of electron attaching gases at low power densities and high pressures.[15,25] At 1100 mTorr, all of the NF_3/Ar discharges collapsed except for the most dilute gas mixture, 18 mol % NF_3/Ar. In all subsequent figures, circled data points represent collapsed discharges.

Impedance measurements of the 86 mol % CF_4/O_2 and 50 mol % C_2F_6/O_2 plasmas are shown in Fig. 4. $|Z_{pe}|$ is shown as a function of pressure in panel (a), while ϕ_{pe} is shown as a function of pressure in panel (b). The pressure dependence of the complex impedance of both the CF_4 and C_2F_6 based discharges are very similar. As the reactor pressure is increased, $|Z_{pe}|$ initially decreases, reaches a minimum and then increases; the smallest values of $|Z_{pe}|$ are observed between 330 and 550 mTorr. At low pressures ϕ_{pe} is strongly negative, but it becomes more positive as the pressure is increased. At the highest reactor pressures ϕ_{pe} becomes inductive (i.e., positive). The highest impedance magnitudes of the CF_4 and C_2F_6 based discharges are significantly lower than the highest impedance magnitudes of the NF_3/Ar discharges; similar results have been reported by Langan *et al.*[11] The C_2F_6 based discharges collapsed only at the highest reactor pressures, 1500 and 2000 mTorr. No collapsed plasmas were observed for any of the CF_4/O_2 discharges. Our results are consistent with impedance measurements of CF_4/O_2 and C_2F_6/O_2 discharges previously reported in the GEC cell.[15,25]

The UE of NF_3 at each reactor pressure is shown as a function of ϕ_{pe} in Fig. 5(a); 5(b) shows the corresponding fluorine atom emission intensity. The most significant feature in Fig. 5 is the presence of maxima in both the UE curve and the fluorine atom emission intensity curve near $\phi_{pe} = -40°$ (i.e., within the transition region). At lower reactor pressures (110 mTorr), increasing the NF_3 partial pressure increases the NF_3 UE and the fluorine atom emission intensity, while at higher reactor pressures (≥330 mTorr) increasing the NF_3 partial pressure decreases the NF_3 UE and the fluorine atom emission intensity. In both the low pressure capacitive and high pressure inductive regions, dimmer plasmas with lower UEs are observed. Throughout the entire experimental matrix the fluorine atom emission intensity appears to mirror the NF_3 UE: higher fluorine atom emission intensities correspond to greater NF_3 UEs. Of particular interest is that changes in the Ar flow rate (i.e., the NF_3 concentration) and the reactor pressure vary the NF_3 UE from 60% to 41%. The rather low emission intensities of the collapsed plasmas are the result of the plasma emission being less efficiently coupled into the spectrometer when the discharge is confined to a small region adjacent to the edge of the powered electrode. The collapsed plasmas have the lowest NF_3 UEs in the entire experimental matrix, presumably because a significant

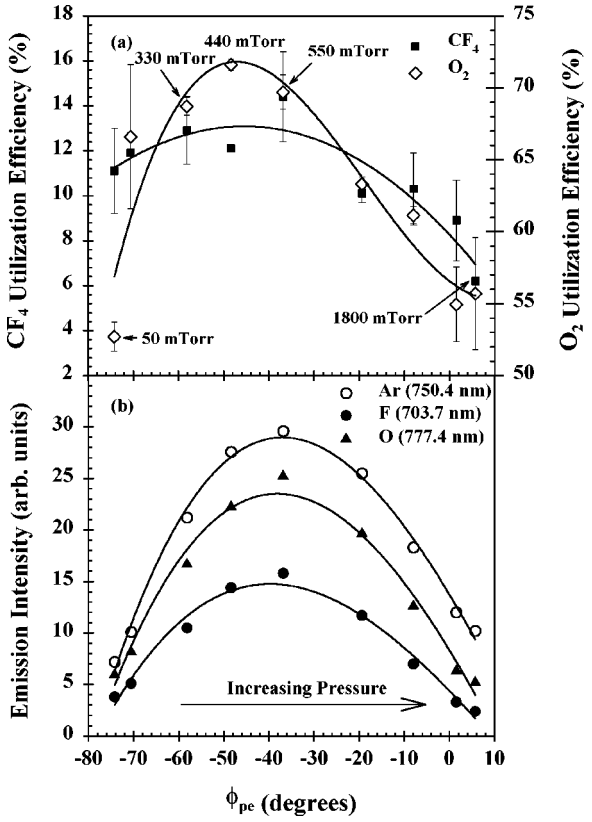

FIG. 6. CF_4 and O_2 utilization efficiencies (a) and baseline corrected fluorine, argon, and oxygen atom emission intensities (b) for the 86 mol % CF_4/O_2 plasmas. Pressures corresponding to selected data points are shown. All data points correspond to a fixed plasma (P_{pe}) of 35.0±0.5 W and 12.5 sccm of CF_4. Cubic or quadratic fits to the data are shown by the solid curves in each panel and meant only as guide for the eye.

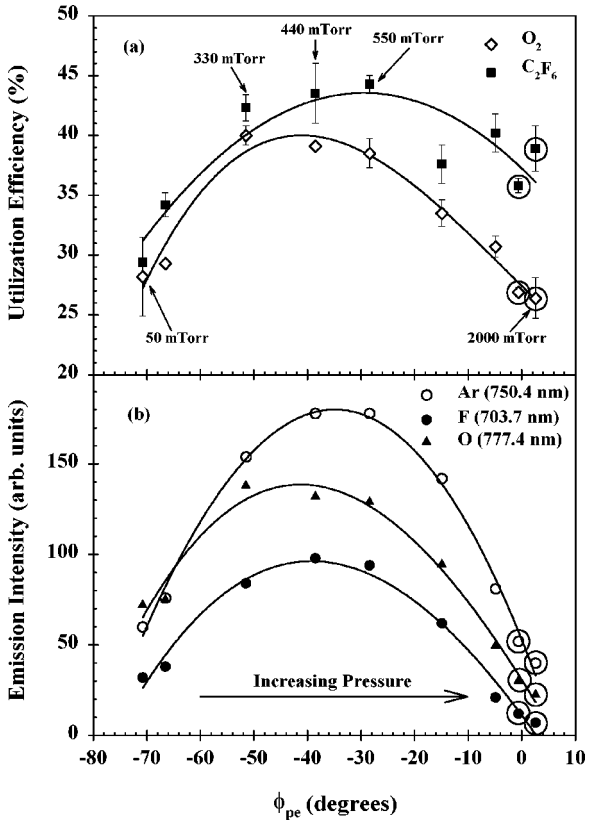

FIG. 7. C_2F_6 and O_2 utilization efficiencies (a) and baseline corrected fluorine, argon, and oxygen atom emission intensities (b) for the 50 mol % C_2F_6/O_2 plasmas. Pressures corresponding to selected data points are shown. The circled data points represent collapsed plasmas. All data points correspond to a fixed plasma power (P_{pe}) of 35.0±0.5 W and 12.5 sccm of C_2F_6. Cubic fits to the data are shown by the solid curves in each panel and meant only as guide for the eye.

fraction of NF_3 can flow directly through the reactor without passing through the small brightly glowing region. The dimmer plasmas with lower UEs observed in the low pressure capacitive region are presumably the result of plasma power being consumed by ions in the powered electrode sheath rather than by electrons in the bulk glow.[15]

The correlation between brighter or more dense plasmas and higher source gas UEs is observed for other electron attaching gases. To illustrate, consider the 86 mol % CF_4/O_2 discharges. Figure 6(a) shows the CF_4 and O_2 UE as a function of ϕ_{pe}, while Fig. 6(b) shows the corresponding fluorine, argon, and oxygen atom emission intensities. The source gas UEs and the atom emission intensities (fluorine, argon, and oxygen) all exhibit a maximum near $\phi_{pe} = -40°$. Smaller O_2 UEs and weaker fluorine, argon, and oxygen atom emission intensities are observed at both lower and higher pressures (i.e., in the low pressure capacitive and the high pressure inductive regions). Interestingly the maximum O_2 UE is shifted towards a more negative phase angle (i.e., a lower pressure) than the maximum fluorine, argon, and oxygen atom emission intensities. However, in general, brighter or more dense plasmas correspond to greater source gases UEs. Note the maximum in the CF_4 UE curve is not sharply defined because the difference between the largest and smallest CF_4 UE is not much larger than the reproducibility of the individual measurements.

Similar behavior is observed for the 50 mol % C_2F_6/O_2 plasmas. Figure 7(a) shows the C_2F_6 and O_2 UEs as a function of ϕ_{pe}, while panel (b) shows the corresponding fluorine, argon, and oxygen atom emission intensities. As observed for the NF_3/Ar and 86 mol % CF_4/O_2 plasmas the source gas UEs (C_2F_6 and O_2) and atomic emission intensities (fluorine, argon, and oxygen) all exhibit a maximum near $\phi_{pe} = -40°$. These maxima all occur between 330 and 550 mTorr. At both lower and higher pressures (i.e., in the low pressure capacitive and high pressure inductive regions) smaller source gas UEs and weaker fluorine, argon, and oxygen atom emission intensities are observed. The maximum O_2 UE and maximum oxygen atom emission intensity both occur at a more negative phase angle than either the maximum C_2F_6 UE or the maximum fluorine or argon atom emission intensities. The collapsed C_2F_6 based plasmas have low source gas UEs.

C_2F_6 plasmas can generate various amounts of CF_4, depending upon the specific process conditions.[1,6] Figure 8 shows flow rate in sccm of plasma generated CF_4 per sccm of C_2F_6 in the 50 mol % C_2F_6/O_2 plasmas, as a function of ϕ_{pe}. The flow rate of plasma generated CF_4 closely tracks the changes in the C_2F_6 UE [Fig. 7(a)]; higher C_2F_6 UEs generate greater amounts of CF_4. Even the lowest C_2F_6 UE observed in this series of experiments (29% at 50 mTorr)

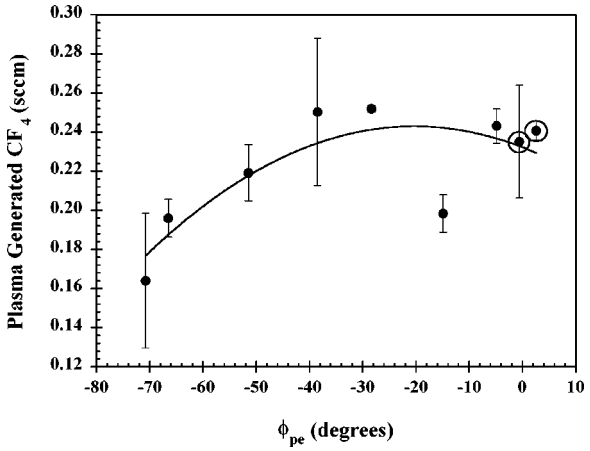

FIG. 8. The rate of production of CF_4 per sccm of C_2F_6 in the 50 mol % C_2F_6/O_2 plasmas. The circled data points represent collapsed plasmas. All data points correspond to a fixed plasma power (P_{pe}) of 35.0±0.5 W and 12.5 sccm of C_2F_6. A quadratic fit to the data is shown by the solid curve and meant only as guide for the eye.

generates 0.16 sccm of CF_4 for each sccm of C_2F_6 fed into the reactor.

Figure 9 shows a plot of the NF_3 UE, in the high pressure inductive and transition regions, as a function of $|I_{ge}|$, where $|I_{ge}|$ is the magnitude of the current flowing from the plasma to the grounded electrode. Operating conditions that favor high currents to the grounded electrode favor high NF_3 UEs. In contrast, operating conditions that have the lowest currents to the grounded electrode (i.e., collapsed plasmas) have the lowest UEs.

Plots of $|I_{ge}|/I_{pe}|$vs ϕ_{pe} for all three gas mixtures (NF_3/Ar, 86 mol % CF_4/O_2, and 50 mol % C_2F_6/O_2) exhibit maxima near $\phi_{pe}=-40°$. Thus within the transition region

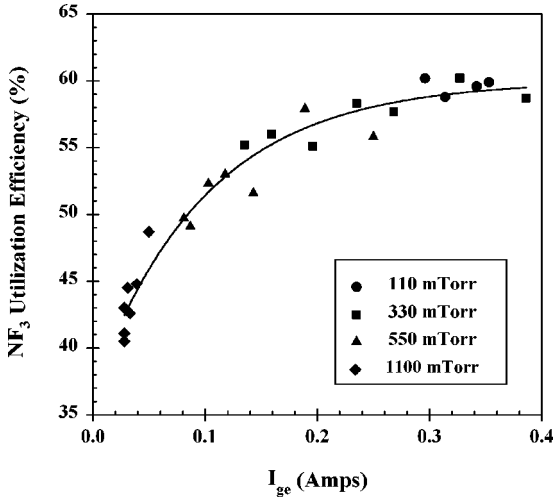

FIG. 9. NF_3 utilization efficiency as a function of the magnitude of the current flowing from the plasma to the grounded electrode (I_{ge}) in the NF_3/Ar plasmas. All data points correspond to a fixed plasma power (P_{pe}) of 35.0±0.5 W and 12.5 sccm of NF_3; at each reactor pressure the mixtures range in composition from 18 to 81 mol % NF_3. A logarithmic fit to the data is shown by the solid curve and meant only as guide for the eye. Not included in this figure are the high Ar flow rate 110 mTorr discharges which show a strong deviation from the depicted trend.

the greatest fraction of current flows to the grounded electrode. Similar results have been reported by Sobolewski *et al.*[15] and Steffens *et al.*[25]

IV. DISCUSSION

Our results clearly show that for every gas mixture investigated in this series of experiments there is a region of minimum discharge impedance and maximum current at the grounded electrode, where the source gas UEs and the atomic emission intensities are maximized. Although the exact operating conditions where this region occurs are specific to a given gas mixture, all gas mixtures investigated exhibited this region within a narrow window of impedance phase angles centered near $\phi_{pe}=-40°$ (i.e., the transition region). The maximum UEs and atomic emission intensities observed near $\phi_{pe}=-40°$ arise from two effects: the increasing absorption of power by ions in the sheath at phases that are more negative, and the contraction and collapse of the discharge at phases that are more positive.

At low total pressures, or low partial pressures of electronegative gas, the phase angle is strongly negative because the discharge impedance is dominated by the capacitive impedance of the sheath at the powered electrode.[15] When the pressure increases, the sheath width and the capacitive impedance of the sheath both decrease. The decrease in the capacitive impedance of the sheath relative to the resistive impedance of the plasma causes the phase to become less negative as the pressure increases. It also causes a greater fraction of the applied voltage to be dropped across the plasma, so that the dc and rf voltages across the sheath decrease. This produces a decrease in the power absorbed by ions in the sheath. Consequently, more of the total plasma power, P_{pe}, is absorbed by electrons in the glow, resulting in greater optical emission intensities and greater UEs. Similarly, if the partial pressure of the electronegative gas is increased at a constant total pressure the electron density in the plasma will decrease, causing the resistive impedance of the plasma to increase relative to the capacitive impedance of the sheath. This results in a shift towards less negative phases, less power absorbed by ions in the sheath, more power absorbed by electrons in the glow, and greater optical emission intensities and UEs. Equations for the power absorbed by ions in the sheath and the power absorbed by electrons in the plasma are reported elsewhere.[15,17,27]

At high total pressures, or high partial pressures of electronegative gas, $|Z_{pe}|$ is large and a different type of behavior is observed. Under these operating conditions, the phase angles are close to zero or positive,[10,11,13,15,16,25] indicating that the resistive or inductive impedance of the bulk plasma dominates the capacitive impedance of the sheaths.[13,15,16] Increasing the pressure, or the partial pressure of the electronegative gas, causes the discharge to become less radially uniform, eventually collapsing into a small ring-like region near the edge of the powered electrode.[15,25] This collapse of the discharge can be explained by impedance arguments.[15] The resistive impedance of the bulk plasma decreases with increasing current density. If the current density along one path increases, the resistance of this path will decrease, causing it

to draw additional current at the expense of other current paths in the discharge.[15] This provides a positive feedback mechanism that eventually results in the collapse of the discharge. As the brightly glowing discharge contracts and eventually collapses, the optical emission intensities, collected from the center of the discharge, are less efficiently coupled into the spectrometer. This accounts for the decrease in the optical emission intensities as the discharge contracts and collapses. Presumably the decrease in UE as the glow contracts and collapses is the result of a large fraction of the feedgas flowing through the reactor without entering the relatively small volume of intensely glowing plasma. Absorption of power by ions in the bulk glow, suggested by the inductive phase angles within this region, may also result in less efficient use of the plasma power for source gas dissociation.[13,15,16]

For each gas mixture the fluorinated source gas UE shows an almost exact correlation with the fluorine atom emission intensity at 703.7 nm. For a fixed argon flow rate, the fluorinated source gas UE also shows an almost exact correlation with the argon atom emission intensity at 750.4 nm. This suggests that in a given plasma reactor the fluorine or argon atomic emission intensity could be used to determine the relative fluorinated source gas UE as operating conditions are varied. Our experiments show that this procedure is valid for fixed NF_3 flow rates or, in the case of CF_4/O_2 and C_2F_6/O_2 discharges, for fixed source gas flow rates. Further experiments would be necessary to verify this procedure for variable fluorinated source gas flow rates. Although the oxygen atom emission at 777.4 nm was also maximized within the transition region, it did not show as strong a correlation with the fluorinated source gas UE for every gas mixture examined.[28]

It is instructive to consider the change in the NF_3 UE as a function of the NF_3 partial pressure, where the NF_3 partial pressure in the reactor is calculated *prior* to initiating a discharge. As shown in Fig. 5 increasing the NF_3 partial pressure (i.e., decreasing the Ar flow rate) at 110 mTorr results in an increase in the NF_3 UE, while increasing the NF_3 partial pressure at higher reactor pressures results in a decrease in the NF_3 UE. This suggests that there is an optimal range of NF_3 partial pressures where the UE is maximized. In our experiments this optimal range of NF_3 partial pressures falls between approximately 50 and 150 mTorr; within this region the discharge impedance is near its minimum value and both the current flowing to the grounded electrode and the fluorine atom emission intensity are near their maximum values. Thus the transition region corresponds to a narrow window of NF_3 partial pressures where the NF_3 UE is maximized. Although the range of NF_3 partial pressures corresponding to the transition region is specific to our reactor and strongly depends upon the operating conditions, the concept of an ideal NF_3 partial pressure may be generally applicable to any plasma reactor constrained to a fixed applied rf power. For example, previous experiments by Langan *et al.* have shown that the maximum etch rates of SiO_2 and Si_3N_4 at different total pressures all occurred at a relatively constant NF_3 partial pressure.[10] Increasing the rf power (P_{pe}) shifts the optimal range of NF_3 partial pressures to higher pressures[15] and increases the NF_3 UE.

As the NF_3 partial pressure increases above 80 mTorr, $|Z_{pe}|$ begins to rapidly increase and, at partial pressures greater than 300 mTorr, becomes extremely large. These large $|Z_{pe}|$'s are consistent with the very electronegative nature of NF_3. At the electron energies commonly found in low temperature discharges, NF_3 has a high dissociative electron capture rate.[29] Dissociative electron capture efficiently sequesters the electrons and creates negative ions in the discharge; even at modest NF_3 partial pressures the negative ion density can be two orders of magnitude greater than the electron density.[26,30] The electron concentration may be further reduced by the formation of molecular fluorine within the plasma,[31] since F_2 also has a large dissociative electron capture rate under similar operating conditions.[32] The low electron concentration and the high negative ion concentration result in very high bulk impedances with significant inductive character.[10–12,16] This accounts for the dramatic increase in the discharge impedance with increasing NF_3 partial pressure. As shown in Fig. 5, these high pressure high impedance conditions result in particularly poor source gas dissociation. Within this region lower NF_3 UEs are observed as the glow contracts as the impedance magnitude increases. The lowest NF_3 UEs are observed when the discharge collapses. In this case a significant fraction of NF_3 can flow directly through the reactor without passing through the small brightly glowing region of the collapsed plasma. Presumably similar reasoning accounts for the decrease in the NF_3 UE as the glow contracts prior to collapsing. Absorption of power by ions in the bulk glow, suggested by the inductive phase angles within this region, may also result in less efficient use of the plasma power for source gas dissociation.[13,15,16] Although the largest $|Z_{pe}|$'s of the CF_4/O_2 and C_2F_6/O_2 plasmas are significantly lower than the largest $|Z_{pe}|$'s of the NF_3/Ar plasmas, the CF_4/O_2 and C_2F_6/O_2 plasmas also exhibit lower UEs at higher impedances.

The argon diluent could also play an active role in determining $|Z_{pe}|$ in NF_3/Ar discharges. For example, in addition to the ionization of Ar atoms, dissociative collisions of Ar metastables and ions with negative ions (F^-) and electron capturing species (NF_3, F_2) may also produce an increase in the free electron concentration in the discharge.[10,11,33–35] Higher electron densities result in brighter or more dense plasmas with lower $|Z_{pe}|$'s and higher NF_3 UEs. These concepts are consistent with the results of Hayashi and coworkers who have shown that the electron density in a NF_3 discharge increases with the addition of Ar.[26] Similar results have been suggested in BCl_3 based plasmas.[35] The addition of Ar to a discharge can also result in changes in the reactive species concentrations due to changes in the electron energy distribution and the average electron energy.[36,37]

The reaction rates for electron-molecule and electron-atom reactions strongly depend upon the electron energy via the excitation cross section for a given reaction.[35,38] For example, the peak dissociative attachment cross section of C_2F_6 ($\sim 1.5\times10^{-17}$ cm^2)[39] occurs at an average electron energy of 3.8 eV while that of O_2 ($\sim 1.4\times10^{-18}$ cm^2)[40] occurs at average electron energy of 6.7 eV. Thus the density

of the electrons capable of a given reaction may change as the electron energy changes. Such differences in the density of electrons of a given energy may account for the fact that the maximum source gas UEs and the maximum atomic emission intensities occur at slightly different values of ϕ_{pe} in different gas mixtures.

Although a number of processes, such as electron impact dissociation, contribute to the consumption of a fluorinated source gas in a discharge, it is interesting to note that the relative UEs of the source gases vary in the same order as the magnitude of their dissociative electron capture rates, at the electron energies commonly found in low temperature discharges.[29,39,40] NF_3 has the largest dissociative electron capture rate[29] and the largest UE, while CF_4 has the smallest dissociative electron capture rate[40] and the smallest UE. In fact the smallest NF_3 UE observed in this series of experiments is just below the maximum C_2F_6 UE and significantly larger than the maximum CF_4 UE. Other investigators have reported significantly higher fluorinated source gas UEs under different operating conditions (e.g., higher applied rf powers, different source gas compositions, etc.).[2,4,6,41–44] However, we expect that the trend in the relative UEs of NF_3, C_2F_6, and CF_4 (NF_3 UE$>C_2F_6$ UE$>CF_4$ UE) should be the same in different plasma reactors under similar operating conditions. For example, in a commercial PECVD reactor Langan *et al.* have reported the relative UEs of NF_3, C_2F_6, and CF_4 vary in the order: $NF_3>C_2F_6>CF_4$.[1]

Previous work has shown that for a fixed applied rf power the power coupling efficiency (the percentage of the available rf power that is dissipated within the plasma) is related to $|Z_{pe}|$in high pressure highly electronegative discharges; higher $|Z_{pe}|$'s result in smaller power coupling efficiencies.[10–14] Thus higher impedance NF_3 based plasmas may have smaller power coupling efficiencies than lower impedance C_2F_6 based plasmas. To illustrate, Langan *et al.* have reported $|Z_{pe}|$, ϕ_{pe}, and P_{pe} for 25 mol % NF_3/Ar and 50 mol % C_2F_6/O_2 discharges in a rf capacitively coupled reactor under similar operating conditions.[11] The higher impedance 25 mol % NF_3/Ar discharge exhibited a significantly lower power coupling efficiency (17%) than the lower impedance 50 mol % C_2F_6/O_2 discharge (>43%). At lower applied rf powers and higher pressures even larger differences would be expected. Thus changes in $|Z_{pe}|$ may not only affect the mechanisms by which power is consumed within a plasma, but can also affect the percentage of available rf power that is dissipated within the discharge. Interestingly, Scofield *et al.* have recently reported that in SF_6/Ar discharges $|Z_{pe}|$was minimized and the power coupling efficiency maximized near $\phi_{pe}=-45°$.[14] This suggests that in an arbitrary plasma reactor either $|Z_{pe}|$or ϕ_{pe} could be monitored to determine the relative fluorinated source gas UE as the operating conditions are varied.

Koike *et al.* have recently reported that for a fixed applied rf power the UE of NF_3, C_2F_6, and CF_4 varied in the order: $C_2F_6>NF_3\gg CF_4$.[6] Since these investigators did not operate at constant plasma power (P_{pe}), their results may differ from ours due to the power coupling efficiency in their reactor. In addition, differences in reactor geometries, diluent concentrations, and the mechanisms by which power is dissipated within the plasma may contribute to the differences between our results. Recall that in our experiments the effects of power coupling efficiencies were eliminated by ensuring that the same amount of power was dissipated within each discharge.

Other investigators have reported that the source gas UE increases as the residence time is increased.[4,44] Smolinsky and Flamm have shown that in CF_4/O_2 plasmas higher CF_4 UEs are obtained for longer residence times.[44] Bruno *et al.* have reported that in neat NF_3 plasmas the UE increases as the residence time is increased.[4] However, in our experiments we do not find that the longest residence times yield the highest source gas UEs. To illustrate, consider the C_2F_6/O_2 discharges. Since the total flow rate is held constant and the pressure is controlled by means of a variable throttle valve, the residence time is directly proportional to the total pressure.[45] As the pressure is increased above 550 mTorr the source gas UEs decrease. For these plasmas the greatest source gas UEs are not obtained at the longest residence times but rather at intermediate residence times corresponding to the transition region (between 330 and 550 mTorr), where the discharge impedance is minimized and the greatest fraction of plasma power is absorbed by the electrons in the bulk plasma. Similar behavior is observed for both the CF_4/O_2 discharges and NF_3/Ar discharges. Differences between our results and those of other investigators are likely due to differences in operating conditions and reactor configurations. We suspect that under appropriate operating conditions these investigators would also observe a decrease in source gas UE with increasing residence time.

Although etch rate experiments were not conducted in this series of experiments, a strong correlation between the fluorine atom emission intensity and the etch rates of SiO_2 and Si_3N_4 in NF_3/Ar discharges has been reported.[10] The etch rates of both materials were found to increase linearly with the fluorine atom emission intensity over a wide range of operating conditions. Since the maximum fluorine atom emission intensity was determined to correspond to the greatest NF_3 UEs in the experiments reported in this article, the same operating conditions may also produce the fastest etch rates of SiO_2 and Si_3N_4 substrates. Previous investigators have shown that in CF_4/O_2 discharges the fluorine atom emission intensity is not strictly proportional to the etch rate of Si.[46,47] Nevertheless, we suspect that the maximum etch rate would occur within or very near the transition region where brightest or most dense plasmas with the maximum CF_4 UEs are observed. Similar results are expected for the C_2F_6/O_2 discharges.

V. CONCLUSION

The operating conditions to achieve the greatest fluorinated source gas UEs in NF_3/Ar, 50 mol % C_2F_6/O_2, and 86 mol % CF_4/O_2 plasmas for a fixed amount of plasma power have been determined, while simultaneously measuring the rf electrical characteristics and optical emission intensities of the plasmas. The UEs in the NF_3/Ar discharges were found to depend on both the reactor pressure and the NF_3 concentration (i.e., the NF_3 partial pressure). The greatest NF_3 UEs

occurred within a narrow range of NF_3 partial pressures corresponding to the brightest plasmas with the lowest impedance magnitudes and the greatest fraction of current flowing to the grounded electrode. The UEs of the 50 mol % C_2F_6/O_2 and 86 mol % CF_4/O_2 plasmas were found to depend on the reactor pressure. The greatest C_2F_6 and CF_4 UEs occurred within a narrow range of reactor pressures corresponding to the brightest plasmas with the lowest impedance magnitudes and the greatest fraction of current flowing to the grounded electrode. Although the operating conditions which resulted in the brightest plasmas with the greatest UEs are specific to a given gas mixture, all gas mixtures investigated exhibited this region within a narrow window of impedance phase angles centered near $\phi_{pe}=-40°$. Within this region, plasma power is most efficiently utilized to dissociate the source gas and excite the atoms that emit light. In lower pressure regions characterized by a capacitive impedance, dimmer plasmas with lower UEs are observed. Presumably this is because the greatest fraction of plasma power is being consumed by ions in the powered electrode sheath rather than by electrons in the bulk glow. Collapsed plasmas, observed for high pressure highly electronegative conditions, exhibited very low UEs. Presumably this is because a significant fraction of the source gas can flow through the reactor without passing through the brightly glowing region, but this may also be the result of absorption of power by the plasma ions. For optimal operating conditions the UE of the fluorinated source gases were found to decrease in the order: $NF_3>C_2F_6>CF_4$.

The practical implications of this work are that the baseline corrected fluorine atom emission intensity (703.7 nm), the magnitude of the discharge impedance ($|Z_{pe}|$), or phase angle of the discharge impedance (ϕ_{pe}) could be monitored to determine the relative fluorinated source gas UE in an arbitrary plasma reactor as the operating conditions are varied. Our results show that these procedures are valid for a fixed NF_3 flow rate, or in the case of CF_4/O_2 and C_2F_6/O_2 based plasmas, for fixed source gas flow rates. The concept of an ideal NF_3 partial pressure could prove to be a useful strategy to prevent the formation of collapsed plasmas at high reactor pressures while maintaining high NF_3 UEs.

[1] J. Langan, P. Maroulis, and R. Ridgeway, Solid State Technol. **39**, 115 (1996).
[2] J. Perrin, J. Meot, J.-M. Siefert, and J. Schmitt, Plasma Chem. Plasma Process. **10**, 571 (1990).
[3] K. Ino, I. Natori, A. Ichikawa, R. N. Vrtis, and T. Ohmi, IEEE Trans. Semicond. Manuf. **9**, 230 (1996).
[4] G. Bruno, P. Capezzuto, G. Cicala, and P. Manodoro, J. Vac. Sci. Technol. A **12**, 690 (1994).
[5] J. P. M. Schmitt, J. Meot, P. Ronbeau, and P. Porrens, *Proceedings of the Eighth European Community Photovoltaic Solar Energy Conference, Florence*, edited by I. Solomon, B. Equer, and P. Helm (Kluwer Academic, Dordrecht, 1988), p. 964.
[6] K. Koike, T. Fukuda, S. Fujikawa, and M. Saeda, Jpn. J. Appl. Phys., Part 1 **36**, 5724 (1997).
[7] P. Maroulis, J. Langan, A. Johnson, R. Ridgeway, and H. Withers, Semicond. Int. **17**, 107 (1994).
[8] B. Anderson, J. Behnke, M. Berman, H. Kobeissi, B. Huling, J. Langan, S.-Y. Lynn, and R. Morgan, Semicond. Int. **16**, 86 (1993).
[9] P. J. Hargis, Jr., K. E. Greenberg, P. A. Miller, J. B. Gerardo, J. R. Torczynski, M. E. Riley, G. A. Hebner, J. R. Roberts, J. K. Olthoff, J. R. Whetstone, R. J. Van Brunt, M. A. Sobolewski, H. M. Anderson, M. P. Splichal, J. L. Mock, P. Bletzinger, A. Garscadden, R. A. Gottscho, G. Selwyn, M. Dalvie, J. E. Heidenreich, J. W. Butterbaugh, M. L. Brake, M. L. Passow, J. Pender, A. Lujan, M. E. Elta, D. B. Graves, H. H. Sawin, M. J. Kushner, J. T. Verdeyen, R. Horwath, and T. R. Turner, Rev. Sci. Instrum. **65**, 140 (1994).
[10] J. G. Langan, S. W. Rynders, B. S. Felker, and S. E. Beck, J. Vac. Sci. Technol. A **16**, 2108 (1998).
[11] J. G. Langan, S. E. Beck, B. S. Felker, and S. W. Rynders, J. Appl. Phys. **79**, 3886 (1996).
[12] J. W. Butterbaugh, L. D. Baston, and H. H. Sawin, J. Vac. Sci. Technol. A **8**, 916 (1990).
[13] H. Kawata, T. Kubo, M. Yasuda, and K. Murata, J. Electrochem. Soc. **145**, 1701 (1998).
[14] J. D. Scofield, P. Bletzinger, and B. N. Ganguly, Appl. Phys. Lett. **73**, 76 (1998).
[15] M. A. Sobolewski, J. G. Langan, and B. S. Felker, J. Vac. Sci. Technol. B **16**, 173 (1998).
[16] H. Shan, J. P. McVittie, and S. A. Self, *Proceedings of the Eight Symposium on Plasma Processing*, edited by G. S. Mathad and D. W. Hess (Electrochemical Society, Pennington, NJ, 1990), Vol. 90-14, p. 229.
[17] Y. T. Lee, M. A. Lieberman, A. J. Lichtenberg, F. Bose, H. Baltes, and R. Patrick, J. Vac. Sci. Technol. A **15**, 113 (1997).
[18] The identification of commercial materials and their sources is made to describe the experiment adequately. In no case does this identification imply recommendation by the National Institute of Standards and Technology nor does it imply that the instrument is the best available.
[19] M. A. Sobolewski, J. Vac. Sci. Technol. A **10**, 3550 (1992).
[20] M. A. Sobolewski, IEEE Trans. Plasma Sci. **23**, 1006 (1995).
[21] A. Johnson, R. V. Pearce, C. A. Schneider, T. W. McGaughey, R. J. Gibson, B. L. Metteer, and R. F. Groves, In Situ Cleaning of Silicon Nitride (Si_3N_4) Process Quartzware Using a Thermal Nitrogen Trifluoride Etch Process; Technology Transfer No. 96083161A-TR; SEMATECH, Austin, TX, 1996.
[22] T. Honda and W. W. Brandt, J. Electrochem. Soc. **131**, 2667 (1984).
[23] Equation (3) assumes that the both rfON signals (I_{SG} and I_{40}) are acquired at a single pressure P_1 and that both rfOFF signals are aquired at a single pressure P_2, however, it does not assume that P_1 and P_2 are equal. It is also assumed that the rfON and rfOFF mass spectra were acquired under identical conditions (i.e., identical amplifier sensitivity, electron multiplier voltage, and mass spectrometer temperature).
[24] Calibration curves for CF_4/Ar mixtures and C_2F_6/Ar mixtures were determined at a fixed total pressure (330 mTorr) and a fixed total flow rate (12 sccm). The $\varepsilon(CF_4/\varepsilon(C_2F_6)$ term was obtained by dividing the reciprocal slope of the $m/e=69$ CF_4 calibration curve by the reciprocal slope of the $m/e=69$ C_2F_6 calibration curve. Both calibration curves were obtained under identical conditions (i.e., identical amplifier sensitivity, electron multiplier voltage, and mass spectrometer temperature) in the absence of a plasma.
[25] K. L. Steffens and M. A. Sobolewski, J. Vac. Sci. Technol. A , **17**, 517 (1999).
[26] T. Hayashi, A. Kono, and T. Goto, Jpn. J. Appl. Phys., Part 1 **36**, 4651 (1997).
[27] V. A. Godyak, R. B. Piejak, and B. M. Alexandrovich, IEEE Trans. Plasma Sci. **19**, 660 (1991).
[28] The 777.4 nm oxygen atom emission intensity in CF_4/O_2 gas mixtures has been attributed to dissociative excitation of O_2 by electron impact; R. E. Walkup, K. L. Saenger, and G. S. Selwyn, J. Chem. Phys. **84**, 2668 (1986).
[29] V. K. Lakdawala and J. L. Moruzzi, J. Phys. D **13**, 377 (1980).
[30] K. E. Greenberg, G. A. Hebner, and J. T. Verdeyen, Appl. Phys. Lett. **44**, 299 (1984).
[31] S. Rauf and M. J. Kushner, J. Appl. Phys. **82**, 2805 (1997).
[32] P. J. Chantry, in *Applied Atomic Collision Physics*, edited by H. S. W. Massey, E. W. McDaniel, and B. Bederson (Academic, New York, 1982), Vol. 3, Chap. 2, pp. 57–59.
[33] R. A. Gottscho and G. Scheller, *Proceedings of the Sixth Symposium on Plasma Processing*, edited by G. S. Mathad, G. C. Schwartz, and R. A. Gottscho (Electrochemical Society, Pennington, NJ, 1987), Vol. 87-6, p. 201.
[34] T. M. Miller, J. F. Friedman, A. E. Stevens Miller, and J. F. Paulson, J. Phys. Chem. **98**, 6144 (1994).
[35] G. R. Scheller, R. A. Gottscho, T. Intrator, and D. B. Graves, J. Appl. Phys. **64**, 4384 (1998).

[36] For example, Dlabal *et al*. have reported that the average electron energy decreases when Ar is added to a dilute NF_3 based plasma; M. L. Dlabal, S. B. Hutchinson, J. G. Eden, and J. T. Verdeyen, Appl. Phys. Lett. **37**, 873 (1980).
[37] G. Oehrlien, in *Handbook of Plasma Processing Technology*, edited by S. M. Rossnagel, J. J. Cuomo, and W. D. Westwood (Noyes, Park Ridge, NJ, 1990), p. 209.
[38] D. L. Flamm, in *Plasma Etching: An Introduction*, edited by D. M. Manos and D. L. Flamm (Academic, New York, 1989), Chap. 2, p. 125.
[39] The peak dissociative attachment cross section of C_2F_6 also depends on the gas temperature. The maximum at 3.8 eV corresponds to a gas temperature of 400 K; L. G. Christophorou and J. K. Olthoff, J. Phys. Chem. Ref. Data **27**, 1 (1998).
[40] L. G. Christophorou, D. L. McCorkle, and A. A. Christodoulides, in *Electron-Molecule Interactions and their applications*, edited by L. G. Christophorou (Academic, New York, 1984), Vol. 1, Chap. 6.
[41] W. W. Brandt and I. Ishii, Proceedings of the Seventh International Symposium on Plasma Chemistry (unpublished), p. 971.
[42] P. J. Hargis, Jr. and K. E. Greenberg, J. Appl. Phys. **15**, 2767 (1990).
[43] J. C. Martz, D. W. Hess, and W. E. Anderson, Plasma Chem. Plasma Process. **10**, 261 (1990).
[44] G. Smolinsky and D. L. Flamm, J. Appl. Phys. **50**, 4982 (1979).
[45] B. Chapman, *Glow Discharge Processes* (Wiley, New York, 1980), p. 16.
[46] C. J. Mogab, A. C. Adams, and D. L. Flamm, J. Appl. Phys. **49**, 3796 (1978).
[47] H. Kawata, T. Shibano, K. Murata, and K. Nagami, J. Electrochem. Soc. **129**, 1325 (1982).